An Improved Scheme for Interpolating between an Atmospheric Model and Underlying Surface Grids near Orography and Ocean Boundaries

Francis Codron, Augustin Vintzileos, and Robert Sadourny

Laboratoire de Météorologie Dynamique du CNRS, Paris, France

ABSTRACT

To take into account the strong nonlinearities of vertical fluxes due to small-scale heterogeneities of surface properties, more and more coupled general circulation models compute part of their atmospheric physical parameterizations, either the surface fluxes or the whole package, on the finer grid of their ocean or land model. A modification of a traditional interpolation scheme is presented to calculate the values of atmospheric variables over surface model grid points. In addition to the desirable properties of flux conservation and preservation of a constant field, the new scheme allows discontinuities in the interpolated fields at the surface model's boundaries and orographic jumps, while remaining continuous elsewhere. It can also be tuned separately for each variable.

The modified scheme is then evaluated using the circulation model of the Laboratoire de Météorologie Dynamique coupled to the Laboratoire d'Océanographie Dynamique et de Climatologie tropical Pacific Ocean model using the delocalized physics method. The results show a large improvement of heat and humidity fluxes near the focus region of the South American coast in the southeastern equatorial Pacific, and a subsequent westward propagation of significant cold SST anomalies.

1. Introduction

Advances in computer power enable global climate models to include more and more components, such as atmosphere, ocean, land, sea ice, and biosphere. Each of these components is often described by a specific model, optimized for its relevant scales and phenomena; thus the component models may have different grids, the atmospheric one generally being the coarsest. For example, the ocean often has a finer resolution, especially at the equator or near the boundaries. The atmosphere has a special role among these climate components because it interacts directly with all the others, the interfacial fluxes providing limit conditions to the underlying surface models in most climate models.

The difficulty comes from the very nonlinear response of the surface fluxes to surface conditions. For example, over the ocean, emitted longwave radiation varies with SST raised to the fourth power. Thus, averaging the surface conditions over an atmospheric grid (AG) box before calculating the fluxes will lead to inaccuracies. To prevent this, several methods are possible, which have in common computing the surface fluxes over the finer surface grid (SG), making a better use of the small-er-scale information. The flux-aggregation method, for instance, based on the work of Claussen (1991a,b) consists in calculating the fluxes in the surface layer over each different surface type, before averaging them with fractional-area weights. This method has been used by Grötzner et al. (1995) in their study of the influence of sea ice inhomogeneities. A similar method is used in the National Center for Atmospheric Research Climate System Model (Bryan et al. 1997). Before calculating the fluxes on the SG grid, the relevant atmospheric variables must be interpolated to it: with flux-aggregation methods only the necessary interfacial variables are calculated, whereas in the delocalized physics approach developed at the Laboratoire de Météorologie Dynamique (LMD), whole atmospheric columns are used (Vintzileos and Sadourny 1997) to take into account the influence of the surface conditions on processes such as convection.

Some discrepancies can however still remain where surface conditions vary abruptly. At the coast for example, there is a strong change from one point to the next in albedo, heat capacity, and roughness length. In summer, this causes a differential heating of the atmosphere over the land and ocean that results, locally, in a sea breeze. Traditional interpolation schemes, often chosen for their continuity properties, do not yield this discontinuity in atmospheric interpolated fields at the SG coastline. The temperature of the lowest atmospheric layer will then tend to be too warm over the ocean, and too cold over land.

Corresponding author address: Dr. Francis Codron, Laboratoire de Météorologie Dynamique du CNRS, Tour 25-15 5 eme etage, Jussieu, CNRS/UPMC, Boite 99, Cedex 05, F-75252 Paris, France. E-mail: francis.codron@lmd.jussieu.fr

This can cause spurious heat fluxes into the ocean and also have indirect effects: the drag coefficient that controls the intensity of the ocean–atmosphere fluxes depends on the wind speed and the thermal stability of the lower atmosphere; an unrealistically high air–sea temperature difference will give very stable conditions, and thus limit evaporation, causing abnormally dry conditions in the atmosphere (Lagarde 1996) and more warming of the ocean. These spurious heat fluxes may be a problem for a realistic climate simulation: not only do they influence directly the SST, but they can also increase the oceanic stratification and thus in some regions limit the cooling of the surface through vertical mixing (Koberle and Philander 1994) or the vertical advection of subsurface anomalies.

Another problem area is near steep orography, like the Andes. Most atmospheric general circulation models use topography-following sigma coordinates near the surface. Then, orography gradients will yield horizontal gradients in variables that have (generally) a monotonic vertical profile, like potential temperature or specific humidity. As the orography will obviously be sometimes steeper in SG than in AG because of resolution differences, the horizontal temperature gradients, for example, should also be stronger.

These considerations lead us to propose a modified interpolation scheme that, while keeping its usual properties over areas of homogeneous underlying surface types, will create the appropriate discontinuities elsewhere. Its principle can be used in various coupling methods, but it has been tested within the delocalized physics scheme, summarized in section 2. The modified scheme is described in section 3 and tested in both one-dimensional experiments and using a coupled Pacific Ocean–atmosphere model (section 4). We conclude in section 5 and discuss its possible applications and extensions.

2. The delocalized physics scheme

In the delocalized physics scheme, the physical parameterizations of the atmospheric model are computed on columns constructed over SG points rather than AG points. The method will be only outlined here, an extensive description can be found in Vintzileos and Sadourny (1997).

From now on, variables and indices defined on the AG will be noted in capital letters, and those on the SG in lower case letters. Before calling the physics package, the atmospheric variables F need to be interpolated over SG columns:

$$f_m = \sum_M I_{mM} F_M, \qquad (1)$$

where m and M are points and the matrix **I** is obviously sparse as influences must be local. The weights must also satisfy

$$\sum_M I_{mM} = 1 \qquad (2)$$

so that a constant field is preserved by the interpolation.

Physical parameterizations are then computed using the f fields, and give vertical fluxes and tendencies g. The surface fluxes can be directly passed to the relevant underlying models, and the whole set of variables must be integrated back to the AG grid. As the g are usually extensive variables, the scheme must be area weighted, and still preserve a constant field:

$$G_M = \frac{\sum_m i_{mM} a_m g_m}{\sum_m i_{mM} a_m}, \qquad (3)$$

where a_m is the area of the SG mesh.

A desirable property would be that two points m and M of the SG and AG grids interact with each other with identical weights, following the action–reaction principle of Vintzileos and Sadourny (1997). This yields $I_{mM} = i_{mM}$.

One last constraint on the weights set is the energy flux conservation: the global energy flux at the surface must be identical on both AG and SG grids, which requires

$$\sum_M A_M G_M = \sum_m a_m g_m. \qquad (4)$$

This is ensured if the coefficients satisfy

$$A_M = \sum_m I_{mM} a_m, \qquad (5)$$

as can be seen by replacing A_M and G_M in (4) by their expressions in (5) and (3), and by using (2). It should be noted that, as the I_{mM} are only locally nonzero, the global energy flux conservation (4) comes from relations that all have a local nature.

Different possible schemes are presented in Vintzileos and Sadourny (1997), along with experiments comparing the delocalized physics to a standard approach.

3. The modified discontinuous interpolation scheme

Whichever interpolation scheme is used, if the coefficients only depend on the relative point locations and not on the different surface types, it will not be able to represent accurately abrupt transitions from ocean to land or orographic contrasts on scales smaller than the atmospheric model mesh size.

a. Description

The proposed solution is basically to keep an accurate scheme, but to give an increased weight to values from AG points with the same surface type as the SG point over which the interpolated fields are calculated.

The starting point is the simple four-point square bilinear interpolation scheme, which yields a set of I_{mM}

TABLE 1. The 1D surface configurations for each value of the horizontal coordinate x. The number given is the altitude of a land point; ''sea'' or ''land'' alone mean altitude 0.

Panel	a	b	c	d	e	f	g	h
$x \leq 50$	Sea	Sea	Sea	$20\,x$	Sea	Land	Sea	Land
$50 < x \leq 75$	Land	400	Sea	$20\,x$	200	200	$40\,(x - 50)$	$40\,(x - 50)$
$75 < x \leq 100$	Land	400	400	$20\,x$	400	400	$40\,(x - 50)$	$40\,(x - 50)$

coefficients. These interpolation coefficients are then modified:

$$I'_{mM} = I_{mM}[1 - \mathcal{H}(m, M)\mathcal{Z}(\sigma)], \qquad (6)$$

where $\mathcal{H}(m, M)$ is a rectification function, equal to 0 when the SG point m is of the same nature as the AG point M, and tending toward 1 when M must not influence m values at all because of extreme surface dissimilarities, for example between ocean and a mountaintop. The function $\mathcal{H}$ will depend on surface types and possibly altitude differences; it may also change with the field to be interpolated as temperature and wind, for instance, do not depend on the same surface conditions in the same way. The function $\mathcal{Z}$, which is altitude dependent, represents the decrease with height of the influence of the surface on the atmospheric profile. Its value ranges from 1 at the surface to 0 at the top of the atmosphere. It can decrease regularly or, more realistically, sharply at the boundary layer top. As is pointed out in the discussion, the function $\mathcal{Z}$ is necessary when flux aggregation is used on more than one vertical level.

The interpolation coefficients must be normalized to satisfy again (2):

$$I''_{mM} = \frac{I'_{mM}}{\sum_{M} I'_{mM}}. \qquad (7)$$

A problem with this scheme arises at the integration level, when the three conditions of energy conservation, invariance of a constant field, and action–reaction cannot be satisfied together, as the I''_{mM} do not satisfy (5). Among these, the action–reaction principle $i_{mM} = I_{mM}$ appears as the least essential to keep: the problematic oceanic SG points near the coast will have f_m values partially extrapolated from neighboring oceanic AG points. This does not mean that the $g_m a_m$ flux should not be integrated to its overlying AG atmospheric column. Thus, the original set I_{mM} will be used for the integration.

b. One-dimensional interpolations

A series of one-dimensional experiments is performed to illustrate how the new scheme functions. The surface grid consists of 100 regularly spaced points between two atmospheric grid points at abscissas 0 and 100; the atmospheric field F is 1 at $x = 0$ and 2 at $x = 100$. The

interpolated field with a simple linear scheme is then $f(x) = 1 + 0.01x$ for any surface configuration.

The new scheme is tested using a set of eight different surface condition distributions listed in Table 1. Both the surface type (ocean–land) and altitude are varying. A function

$$\mathcal{H}(x, i) = \begin{cases} d\varphi(x, i)/[1000 + d\varphi(x, i)] \\ \quad \text{for same surface type} \\ 0.5\{1 + d\varphi(x, i)/[1000 + d\varphi(x, i)]\} \\ \quad \text{for different surface types} \end{cases} \qquad (8)$$

is used, where $d\varphi(x, i)$ is the absolute value of the geopotential difference between SG point x and AG point i. The weight of an atmospheric land point is thus divided at least by two in the interpolation over an oceanic point.

The results are displayed in Fig. 1. Figure 1d confirms that for a smooth topography, the interpolated field $f(x)$ is unchanged from the linear scheme. Otherwise, f is monotonic and discontinuous at the coast and at abrupt changes in topography. Comparison between Figs. 1e and 1f, and 1g and 1h, shows that the gap is greater when there is an ocean–atmosphere contrast in addition to an altitude jump. These were the desired characteristics for the new scheme.

4. Validation experiment

The new scheme has been tested using the LMD atmospheric GCM coupled to the Laboratoire d'Océanographie Dynamique et de Climatologie (LODYC) tropical Pacific Ocean model OPA6 with the delocalized physics method. The version LMD-5b of the atmospheric model is close to the one used by Harzallah and Sadourny (1995), and its main features are summarized in Table 2. The LODYC grid over the tropical Pacific has a much higher resolution (228×94 points from $120°$ to $290°$E and from $40°$S to $48°$N) than the atmospheric grid. A 30-yr run of the coupled model is described in Vintzileos et al. (1999a,b).

A control experiment (run STD) uses the standard four-point bilinear interpolation scheme, slightly different from the six-point second-order scheme used in the validation experiments from Vintzileos and Sadourny (1997). The results with either scheme are very similar, but the discontinuous scheme is easier to implement in a four-point context. The modified discon-
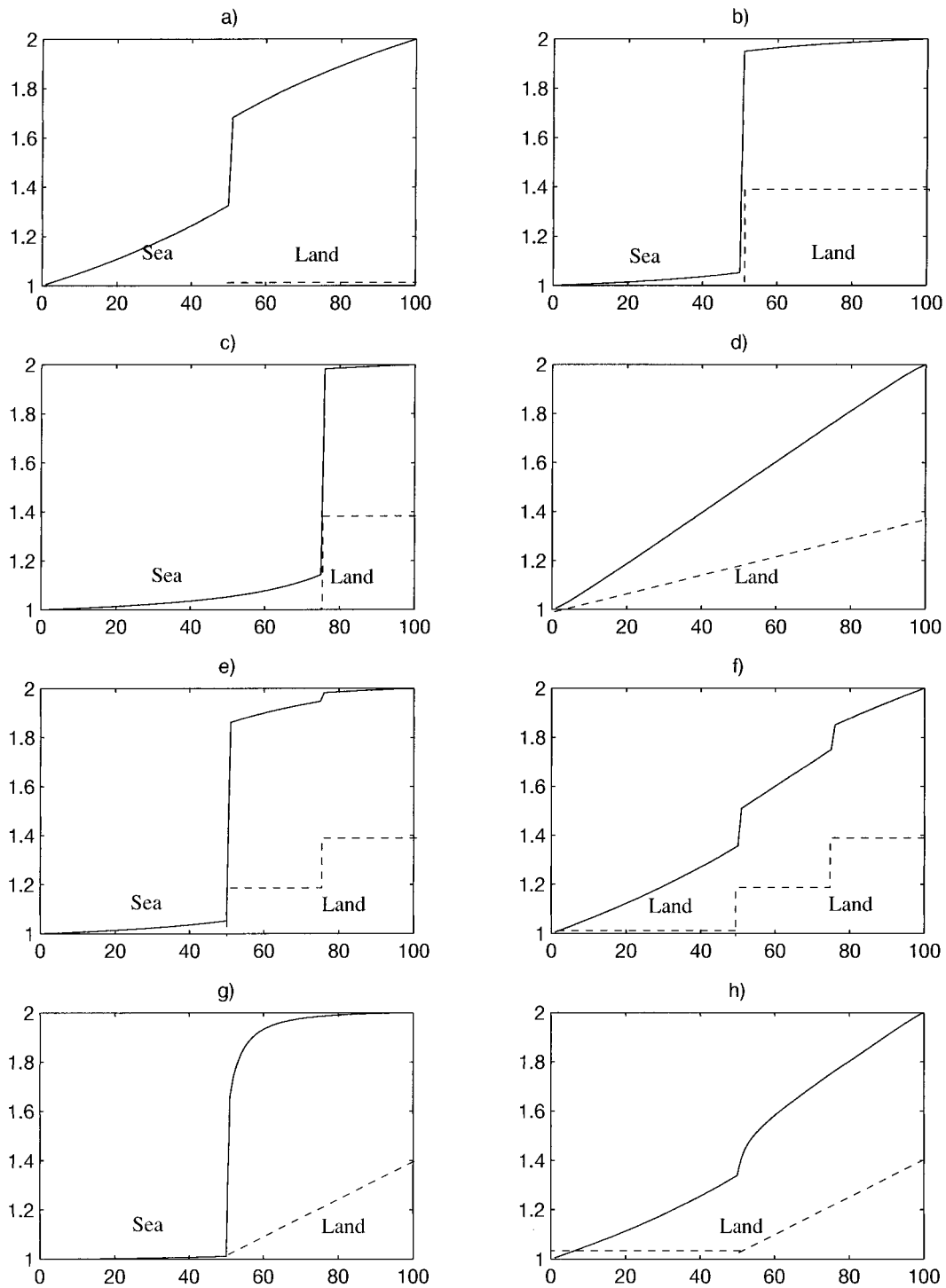
FIG. 1. The 1D interpolated field F (ordinates). The surface conditions profiles for $1 \leq x \leq 100$ (abscissas) for each panel are given in Table 1, and a sketch is drawn in discontinuous lines.

tinuous interpolation scheme is used in a sensitivity experiment (run DIS) for all atmospheric variables except the wind, to allow an easier interpretation of the fluxes changes. The Z function is proportional to $\sigma = p/p_0$ and thus decreases exponentially with height.

a. Two-dimensional interpolations of surface fields

The focus will be on the southeastern Pacific area. This region appears quite crucial for the tropical Pacific climate, and its realistic simulation is essential. Very

TABLE 2. LMD-5b Atmospheric GCM characteristics.

Horizontal resolution	64 longitude $\times$ 50 sin (latitude)
Dynamic equations	Sadourny (1975)
Lateral diffusion	Bi-Laplacian
Vertical coordinate	11 layers in $\sigma = p/p_s$
Thermodynamical variable	Potential enthalpy $H = C_p T(p_s/p)^\kappa$
Shortwave radiation	Fouquart and Bonnel (1980)
Longwave radiation	Morcrette (1991)
Cloud parameterization	Le Treut and Li (1991)
Boundary layer	Bulk aerodynamic
Convection schemes	Manabe and Strickler (1964) saturated case; Kuo (1965) unsaturated case

sharp ocean–land contrasts are also found here near the Andes, making it a good testing place for the problem studied. To isolate the effect of the change of interpolation scheme, the different fields are first studied on the first coupling time step, after half an hour of simulation. The variables are thus identical for all runs on the AG grid before the interpolation, as is the SST. The date is 1 January, in the Southern Hemisphere summer.

Figure 2 shows the potential temperature $\theta = T(p_s/p)^\kappa$ on the lowest atmospheric layer, interpolated with the standard (Fig. 2a) and modified (Fig. 2b) schemes. With the standard scheme, the expected high θ over land leads to a high temperature over some oceanic regions, whereas with the new scheme there are only weak gradients of θ all over the ocean, except near the coast at 25°S. Here, there is a coastal plain, and the lack of a topographic step reduces the discontinuity in the interpolated field. The DIS field appears more realistic, as the high values of θ in STD are mainly artifacts due to the coarse AG resolution. This is made very clear by Fig. 2c, which shows the difference between the two runs. The contours of the θ difference follow closely the AG boundaries. The resulting ocean–atmosphere sensible heat flux difference shown in Fig. 2d reaches 50 W m^{-2}, the heat flux being positive when from the ocean into the atmosphere.

To study the effects on evaporation, it is necessary to discriminate between the two mechanisms discussed in the introduction: changes of the interpolated water vapor field, and of the drag coefficient through differences of the thermal stability of the lower atmosphere (the wind at the first time step is identical in both runs). So, we did a third experiment DISQ where only the liquid water and water vapor fields were interpolated with the new scheme. The drag coefficient is thus the same in STD and DISQ. The results are displayed in Fig. 3. The mixing ratio is generally higher in DISQ near the coast, the air being drier over land. The evaporation is lower in DISQ (Fig. 3b), thus mostly warming the ocean. However, this effect is canceled by the changes in the drag coefficient. Figure 3c shows the difference between runs DIS and DISQ, which have the same mixing ratios but different air temperatures. The air–sea temperature difference is much lower in DIS, and the

resulting instability increases the evaporation. The net effect on the latent heat flux is thus of the same sign and magnitude as the one on the sensible heat flux.

Figure 3d shows the total difference in sensible and latent heat flux between the two schemes. It is everywhere positive near the coast and reaches 100 W m^{-2} at latitudes between 25° and 40°S where the insolation is highest at the date studied, a value that is comparable to the mean total energy flux.

b. Coupled simulations

In a long coupled run, these lower heat fluxes into the ocean will lead to colder SSTs, which will in turn increase back the fluxes. A new equilibrium should be reached, with various feedback mechanisms also intervening. A complete analysis is however beyond the scope of this paper, and only some basic fields will be shown.

Figure 4 shows the mean SST for the Comprehensive Ocean–Atmosphere Data Set (COADS) (Oberhuber 1988), to compare with the first 5-yr-average SST in the STD and DIS runs (Figs. 5a,b) and their difference (Fig. 6). The standard run SST has anomalous warm patches at several places near the eastern Pacific coast that are much weaker in DIS. The new scheme produces SSTs that are several degrees colder near the coast. Interestingly, the new scheme also produces a region of SSTs that are 0.5° colder than the STD run that is confined to the equator and extends to 120°W in the cold tongue region. These results are very robust when the duration of the analysis is changed and do not display a strong seasonal cycle off the coast. This 0.5° difference can affect the behavior of the model through the change of the mean zonal and meridional SST gradients, or changes in the stability of the upper oceanic layers near the eastern Pacific coast. To give an idea of the importance of a 0.5° difference, the standard deviation of the mean SST in the Niño-3 box for a 30-yr standard run is 0.38°C, and 0.3°C for interannual anomalies.

Both the STD and DIS runs compare reasonably well to the COADS observations, the main defaults being a cold tongue too narrow and penetrating too far in the west, and too warm SSTs in the east. The changes between the two runs show an improvement in the widening of the cold tongue in the east and the cooling at the coast.

5. Conclusions and discussion

A new scheme that takes into account the presence of different underlying surface types has been proposed for the interpolation of atmospheric model variables onto a finer surface grid. As demonstrated by simple 1D experiments, the interpolated fields are continuous at the atmospheric mesh boundaries, but may be discontinuous where the surface conditions are, yielding more realistic profiles.
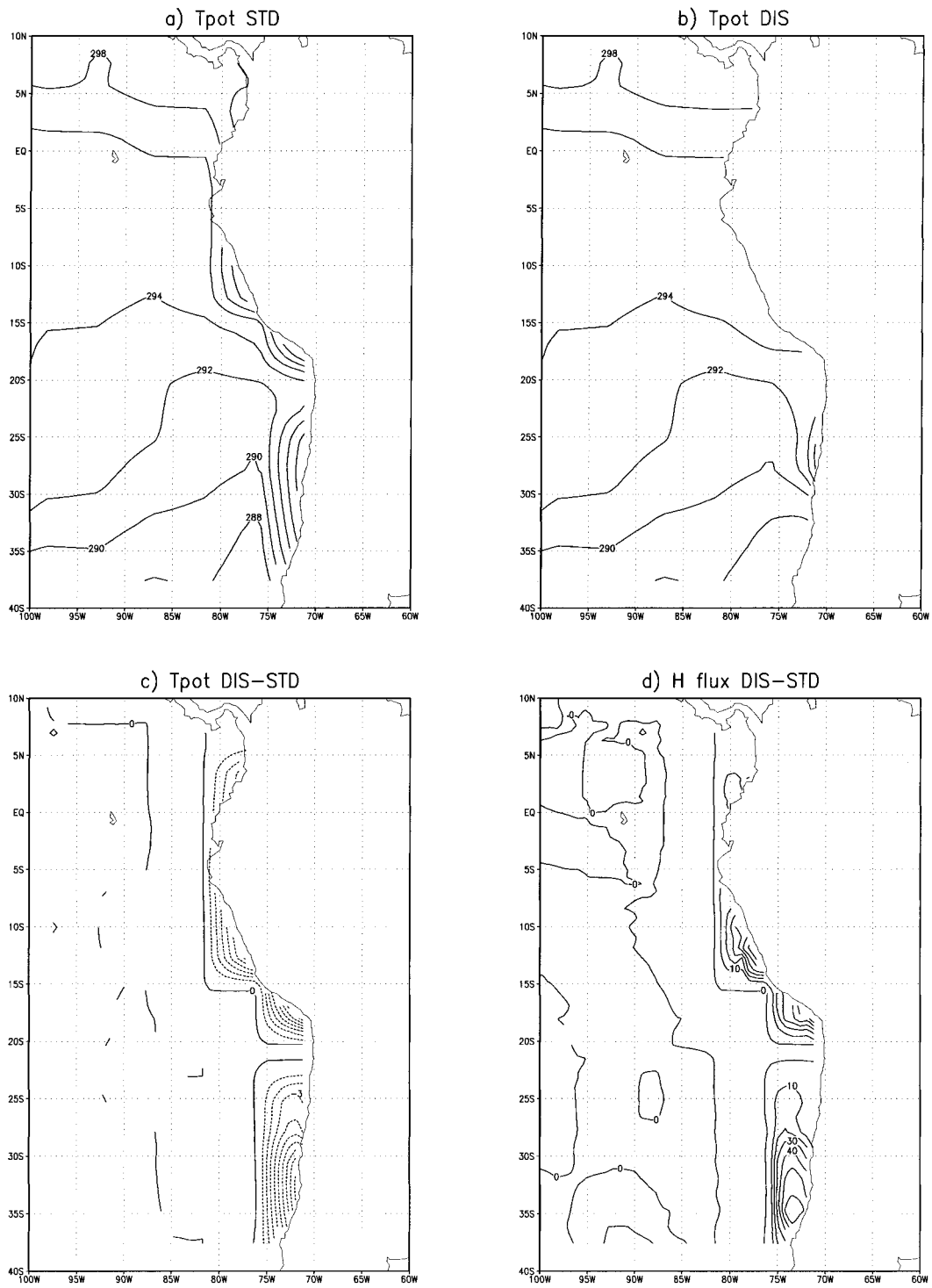
FIG. 2. Potential temperature at the first atmospheric level interpolated over the SG grid at the first time step. (a) STD run, (b) DIS run with discontinuous scheme at the coast. (c) DIS–STD difference. (d) DIS–STD ocean to atmosphere sensible heat flux difference in W m^{-2}.
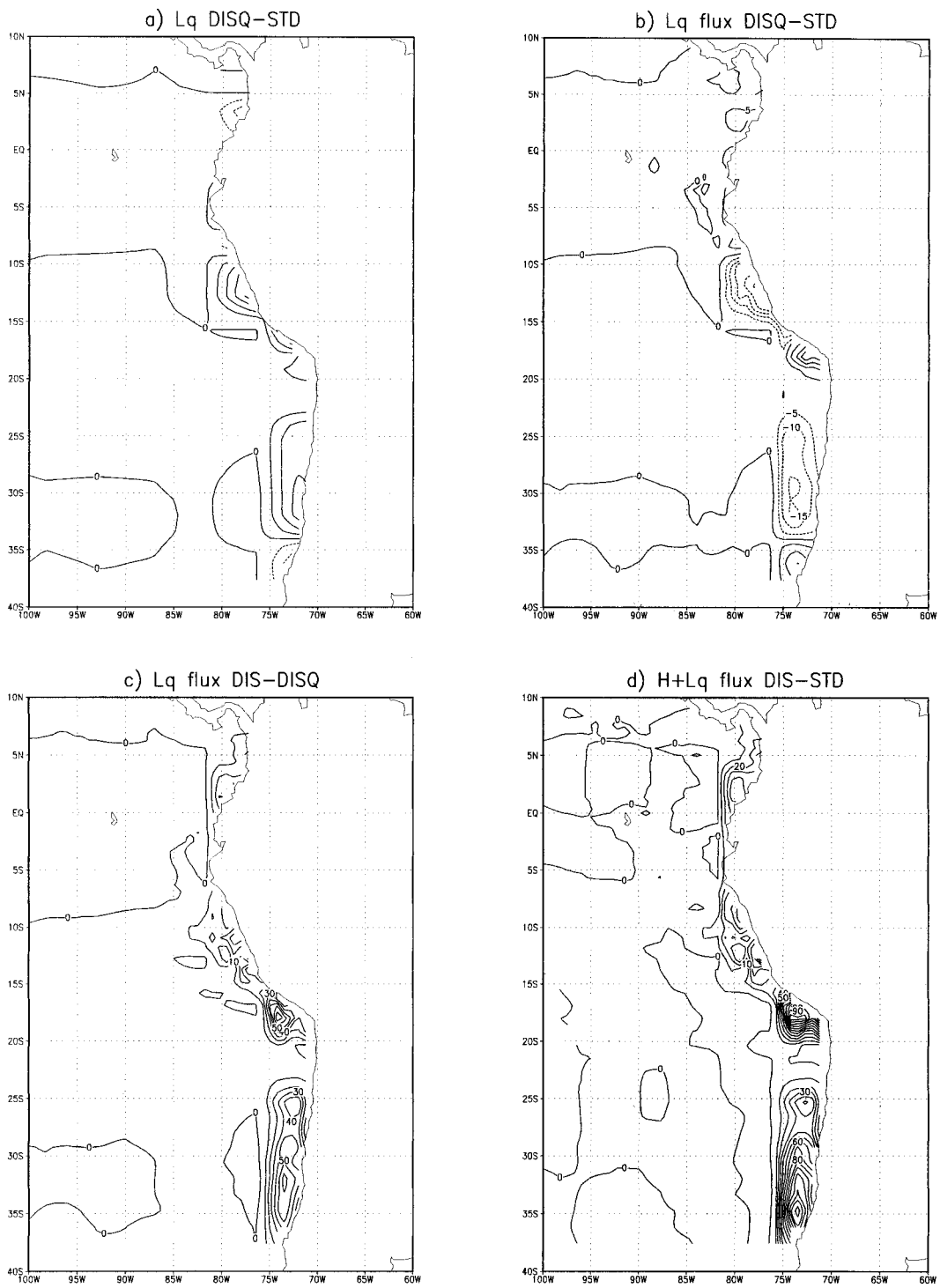
a) Lq DISQ-STD

b) Lq flux DISQ-STD

c) Lq flux DIS-DISQ

d) H+Lq flux DIS-STD

FIG. 3. Latent heat content and flux on the first atmospheric layer (fluxes are positive from the ocean to the atmosphere). (a) DIS–STD latent heat content difference (in J kg^{-1}). (b) DISQ–STD (same drag coefficient) latent heat flux in W m^{-2}. (c) DIS–DISQ (same specific humidity) latent heat flux. (d) Total DIS–STD latent and sensible heat flux.
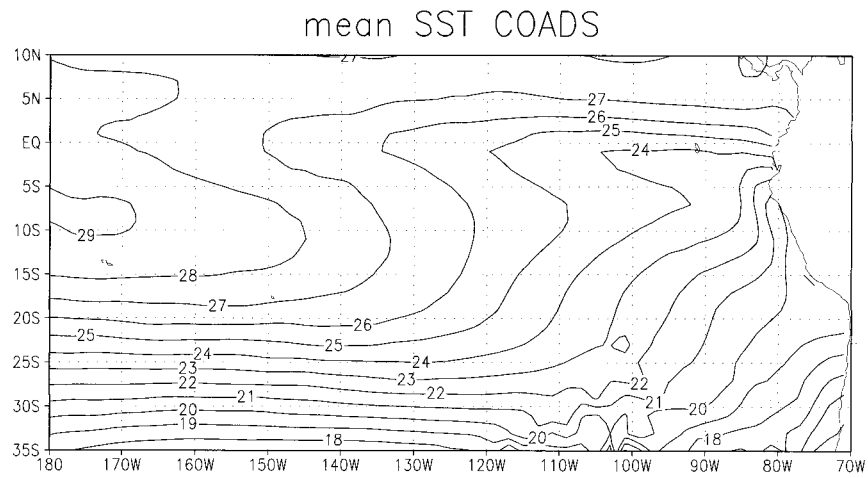
mean SST COADS

FIG. 4. Mean SST in the Oberhuber (1988) COADS observations dataset.

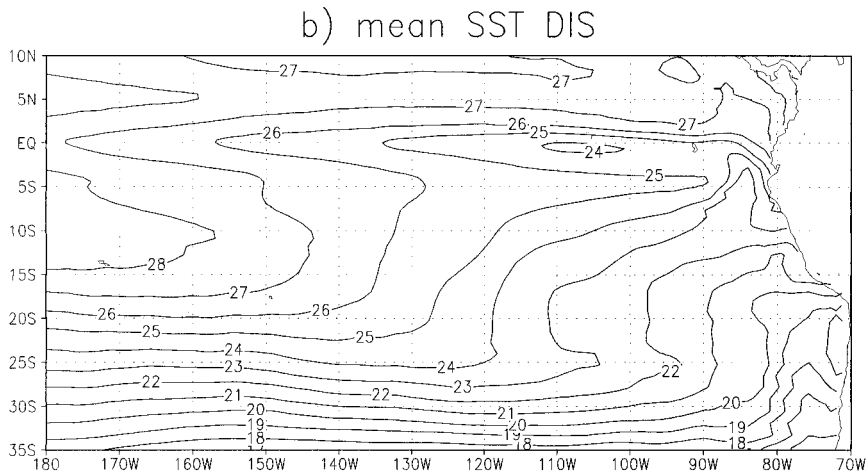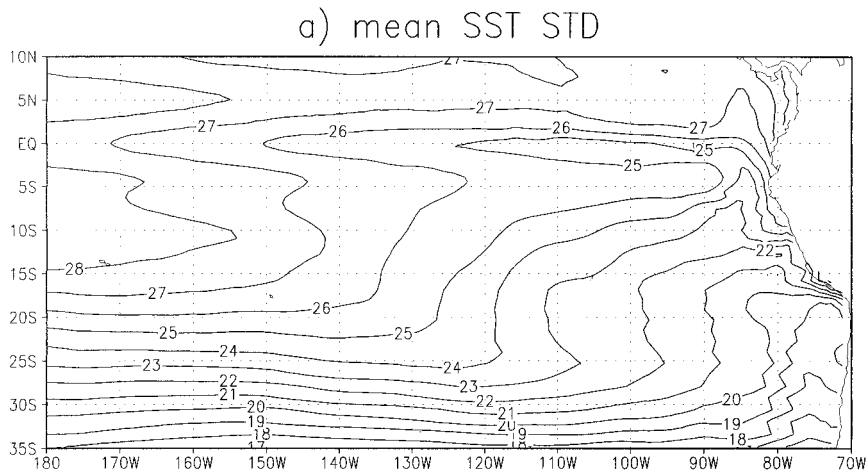## a) mean SST STD

b) mean SST DIS

FIG. 5. The 5-yr mean SST, coupled model runs: (a) STD run, b) DIS run.
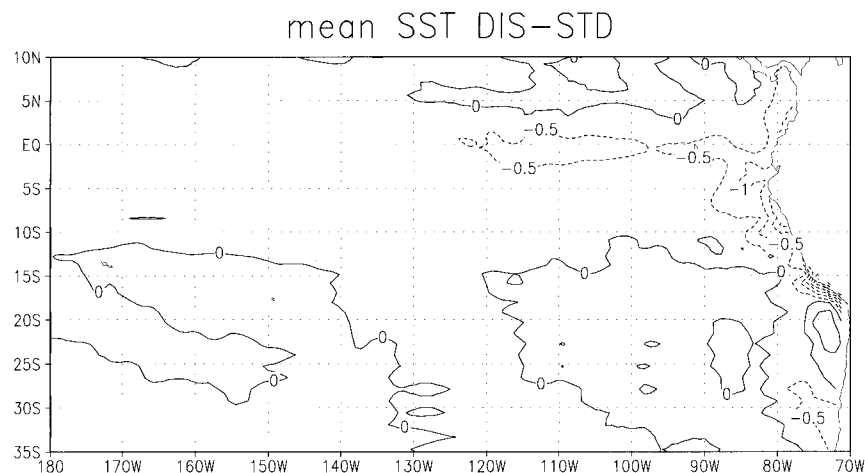
FIG. 6. The 5-yr mean SST difference in the DIS–STD coupled runs.

This new scheme has been successfully tested for the temperature and specific humidity on a coupled atmosphere–Pacific Ocean general circulation model using the delocalized physics method. Important discrepancies near the eastern Pacific coast in sensible and latent heat flux have been corrected. Both the temperature and humidity differences in the lowest layer, and the changes in the drag coefficient due to differences in the vertical stability, were involved. This is quite important, as the near-equatorial Pacific is a very sensitive area: localized anomalies can easily propagate and amplify through coupled mechanisms between the SST and zonal wind. Indeed, significant differences in the SST were also observed far off the coast in the equatorial cold tongue area, showing that the consequences are not only local.

Discontinuous interpolation versus extrapolation: A solution used by several current coupled models to avoid unrealistic air temperatures and heat fluxes over the ocean near the coasts is to extrapolate the values from neighboring AG oceanic points. This may prevent the most obvious problems, but appears quite crude: to calculate a profile over an oceanic SG point, either only, or no information from, AG land points must be used. The discontinuous interpolation scheme can be reduced to an extrapolation by taking $\mathcal{H}$ and $\mathcal{Z}$ equal to 1, but the use of these two functions provides additional flexibility.

The $\mathcal{H}$ function enables the scheme to keep some information from the AG land points, and to change the strength of the contrast for different variables and different surface type transitions. For example, the temperature or water content contrast should be greater at an ocean–desert coastline than for an ocean–swamp-like transition. The altitude difference between two adjacent points is also included in $\mathcal{H}$, which can be quite important. Schneider et al. (1997) for example found that an extrapolation of the wind near the eastern coasts of equatorial oceans significantly improves their coupled model; however this extrapolation should be stronger

near steep orography where it is more physically justifiable.

The function $\mathcal{Z}$ is also important for models that use flux aggregation on whole atmospheric columns and not only on the first layer. Here, the vertical fluxes and radiative transfers are calculated in columns covering the SG meshes, then integrated to the AG grid. Extrapolating atmospheric profiles over the problematic SG points supposes that the influence of the surface conditions fully extends to the top of the atmosphere. This is obviously not true, so the extrapolation will yield wrong vertical profiles and, thus, wrong fluxes. On the other hand, $\mathcal{Z}$ allows a more realistic modulation of this influence with the altitude: it can, for example, decrease above a prescribed or calculated mixed layer top.

Special cases: Some coupled models compute the atmospheric physical parameterizations separately over land and ocean at the coast, where an AG mesh covers both surface types, but use averaged surface conditions elsewhere. This is the case, for example, in the double physics method tested at the European Centre for Research and Advanced Training in Scientific Computation (Lagarde 1996). They encountered the same type of problems: too high air temperatures over the sea near the coast leading to a lack of evaporation through increased stability. The solution would be to attribute different coordinates to the two columns constructed from one AG mesh point, which should be approximately those of the barycenter of the oceanic and continental parts. The discontinuous interpolation scheme can then be used to calculate appropriate values for the atmospheric fields over each column.

An extreme case is an island smaller than an AG mesh. For the scheme to work, this island must be represented by a land point in the AG grid. The fluxes can then be calculated separately over the island and the neighboring ocean using the method described above. It is necessary that the island is represented as land in the AG grid, so that the interpolation scheme can use

the difference in surface conditions. The case of a big lake or inland sea is exactly similar, but reversed: it must exist as sea in the AG grid for the scheme to work.

The discontinuous interpolation scheme can thus be introduced in models using a great variety of coupling methods and will improve the interfacial fluxes calculation near water–land boundaries and steep orography, with almost no additional computational cost. There remain however some problems: first, the scheme cannot represent nonmonotonic horizontal profiles, like a succession of hills. However, actual global coupled models generally do not represent such subgrid details over land. The main difficulty is when different surface types are defined as fractional areas of a mesh with no specific location, as with the sea ice–open sea difference. The air should be warmer over open water than over sea ice, but all AG meshes in a given area can have similar sea ice proportions, making the discontinuous scheme ineffective as there is no surface type difference among the AG points. Another solution will have to be found, perhaps by storing different vertical profiles over different surface types.

REFERENCES

Bryan, F., B. Kauffman, W. Large, and P. Gent, 1997: The NCAR CSM flux coupler. NCAR Tech. Rep. NCAR/TN-424 + STR, Boulder, CO, 49 pp.

Claussen, M., 1991a: Local advection processes in the surface layer of the marginal ice zone. *Bound.-Layer. Meteor.,* **54,** 1–27.

——, 1991b: Estimation of areally-averaged surface fluxes. *Bound.-Layer. Meteor.,* **54,** 387–410.

Fouquart, Y., and B. Bonnel, 1980: Computation of solar heating of the earth's atmosphere: A new parametrization. *Beitr. Phys. Atmos.,* **53,** 35–62.

Grotzner, A., R. Sausen, and M. Claussen, 1995: The impact of subgrid scale sea-ice inhomogeneities on the performance of the atmospheric general circulation model ECHAM3. *Climate Dyn.,* **12,** 477–496.

Harzallah, A., and R. Sadourny, 1995: Internal versus SST-forced atmospheric variability as simulated by an atmospheric general circulation model. *J. Climate,* **8,** 474–495.

Koberle, C., and S. G. H. Philander, 1994: On the processes that control seasonal variations of sea surface temperatures in the tropical pacific Ocean. *Tellus,* **46A,** 481–496.

Kuo, H., 1965: On formation and intensification of tropical cyclones through latent heat release by cumulus convection. *J. Atmos. Sci.,* **22,** 40–63.

Lagarde, T., 1996: Double physique, documentation informatique. Tech. Rep. I.M. 94, CERFACS, 16 pp. [Available from CERFACS, 42, Avenue Coriolis, 31057 Toulouse, France.]

Le Treut, H., and Z.-X. Li, 1991: Sensitivity of an atmospheric general circulation model to prescribed SST changes: Feedback effects associated with the simulation of cloud optical properties. *Climate Dyn.,* **5,** 175–187.

Manabe, S., and R. Strickler, 1964: Thermal equilibrium of the atmosphere with a convective adjustment. *J. Atmos. Sci.,* **21,** 361–385.

Morcrette, J. J., 1991: Radiation and cloud radiative properties in the ECMWF operational weather forecast model. *J. Geophys. Res.,* **96,** 9121–9132.

Oberhuber, J. M., 1988: An atlas based on the COADS dataset: The budgets of heat, buoyancy and turbulence kinetic energy at the surface of the global ocean. MPI Tech. Rep. 15, Max-Planck-Institut, Hamburg, Germany, 199 pp.

Sadourny, R., 1975: The dynamics of finite-difference models of the shallow-water equations. *J. Atmos. Sci.,* **32,** 680–689.

Schneider, E., Z. Zhu, B. Giese, B. Huang, B. Kirtman, J. Shukla, and J. Carton, 1997: Annual cycle and ENSO in a coupled ocean–atmosphere general circulation model. *Mon. Wea. Rev.,* **125,** 680–702.

Vintzileos, A., and R. Sadourny, 1997: A general interface between an atmospheric general circulation model and underlying ocean and land surface models: Delocalized physics scheme. *Mon. Wea. Rev.,* **125,** 926–941.

——, P. Delecluse, and R. Sadourny, 1999a: On the mechanisms in a tropical ocean–global atmosphere general circulation model. Part I: Mean state and the seasonal cycle. *Climate Dyn.,* **15,** 43–62.

——, ——, and ——, 1999b: On the mechanisms in a tropical ocean–global atmosphere general circulation model. Part II: Interannual variability and its relation to the seasonal cycle. *Climate Dyn.,* **15,** 63–80.